Crystallography and Spectral Analysis in structuring of 7,8-dihydroxy-4-Phenyl Coumarin Monohydrate

C. N. Dipunadas and V. Bena Jothy

Department of Physics and Research Centre,
Women's Christian College, Nagercoil, Tamil Nadu, India-629 001

**Corresponding author E-mail*: dipunaabynraj@gmail.com

(Received 28 October 2017, Accepted 05 December 2017, Published 16 December 2017)

Abstract

Vibrational assignments of 7,8-dihydroxy4-phenyl coumarin monohydrate have been made both in crystalline and gas phase. Infrared absorption and Raman spectra of 7,8-dihydroxy4-phenyl coumarin monohydrate have been interpreted and compared by electronic structure calculations at B3LYP using 6-311++G(d,p) basis set. Down-shifting of frequencies of O-H vibrations due to intra-molecular O-H…O hydrogen bonding as well as inter-molecular interactions with solvent molecule were resolved by NCA analysis. Sharpness of endothermic peak in TG/DTA shows the good degree of crystallinity and purity of the sample.

***Keywords*:** Neoflavonoid, FT-IR & FT-Raman, DFT, TG/DTA.

1. Introduction

Coumarin, with a benzopyrone framework is structurally constructed by a phenyl ring fused to α-pyrone ring that possess conjugated system with rich electron and good charge transfer properties [1,2]. Coumarin compounds as medicinal drugs attracted special interest due to their potential biological activities such as antibacterial, anti-inflammatory, antioxidant, anti-tumour activity [3-6] and also identified as protease and integrase inhibitors[7,8]. Veselinović et al. [9] reported that 4-phenyl hydroxycoumarins can be considered as good molecular templates for potential antibacterial agents. Various structural derivatives of 6-hydroxycoumarin and 7-hydroxycoumarin synthesized by Koketsu et al. [10] have been reported as effective agents for relieving symptoms of inflammation. Spectral behavior of the optimized structures of 4-hydroxycoumarin compounds was

reproduced by the hybrid DFT methods B3LYP and B3P86 with 6-31G** and aug-cc-pVDZ basis sets[11]. Normal coordinate calculations of 7-hydroxycoumarin have been carried out using Wilson's FG Matrix mechanism on the basis of General Valence Force Field (GVFF) for both in-plane and out-of-plane vibrations [12].

Flavonoid compound 7,8-dihydroxy-4phenyl coumarin monohydrate (DHPC) belongs to neoflavonoid family having C3-C4 double bond and 4-phenyl chromene backbone. Spectroscopic techniques along with density functional theory (DFT) computations have achieved substantial interest in determining molecular structural elucidation, physical and chemical properties leading to the bioactive nature of the compound. This article highlights the hydrogen bonding interactions confirmed by both crystallographic and spectral analytical techniques supported by density functional (DFT) computational methods. Thermal behavior about sample with an inert reference as a function of increasing temperature undergoing identical thermal cycles via thermogram and differential thermal analysis (TG-DTA) analysis have been predicted.

2. Experimental Details

Bruker AXS Kappa Apex2 CCD single crystal X-ray diffractometer was used to find the crystal structure of DHPC. FT-IR spectrum of DHPC was recorded in the region 4000-400cm^{-1} using Perkin Elmer spectrophotometer with the spectral resolution of 1cm-1 while FT-Raman spectrum of DHPC was recorded in the region 4000-50 cm^{-1} using Bruker RFS 27 spectrophotometer using 1064 nm excitation from an Nd:YAG (neodymium-doped yttrium aluminium garnet) laser source with the spectral resolution of 2 cm-1. Thermal analytical studies of DHPC were carried out by using a SDT Q600 V20.9 Build 20 in an inert nitrogen atmosphere.

3. Computational Details

ORTEP 3 [13-14] and Mercury 3.9 [15] are an excellent visualization tools for crystallographic structural analysis. Structural refinement details and crystal data of grown crystal of DHPC were obtained using publcif. Unit cell parameters were determined by least-square technique using many reflections and the structure solved was further refined by full-matrix least squares method using SHELXL97 [16]. Geometry optimization and wavenumber assignments were performed using Becke-3-Lee-Yang-Parr (B3LYP) gradient correlation functional with 6-311++G(d,p) the basis set [17-20] using Gaussian 09W program package developed by Frisch and coworkers [21]. Scaling factor (0.9673) [22,23] for corresponding basis set in order to correct the theoretical errors, such as electron correlation and basis set deficiencies caused by neglecting anharmonicity while potential energy distribution (PED) for the normal modes were computed using MOLVIB 7.0 program [24,25]. To improve the agreement between predicted and observed wavenumbers, computed harmonic wavenumbers were scaled according to the scaled quantum mechanical force field (SQMFF) procedure [26]. Deviation from the experiments after scaling was found to be less than 9 cm-1 with a few exceptions. Descriptions of the predicted wavenumbers during the scaling process

were followed by potential energy distribution matrix and Cartesian representation of force constants were transferred to a non-redundant set of symmetry coordinates, chosen in accordance with the recommendations of Pulay et al. [27,28]. Perl script called thermo.pl extracted the essential data from a Gaussian output file and compute thermodynamic functions at several temperatures [29].

4. Results and Discussion

4.1 Recrystallization process

Powdered form of 7,8 dihydroxy 4-phenyl coumarin monohydrate with a stated purity of greater than 98% was purchased from Sigma Aldrich Company, India. Methanol was used as solvent for recrystallization process in order to reproduce crystal sample. Solution saturates over a period of 20 days and small needle shape grown crystals with crystal size of 0.30 x 0.25 x 0.20 mm^3 was used for further studies.

4.2 X-Ray crystallography

From the crystal data and structure refinement of DHPC shown in Table1, it is found that final anisotropic full-matrix least-squares refinement on F^2 with 778 variables converged at *R1* = 5.65%, for the observed data and *R2* = 19.98% for all data. The goodness-of-fit was 1.153. The largest hole was -0.241 e/$Å^{-3}$ with an RMS deviation of 0.029 e/$Å^{-3}$ and based on the final model, the calculated density was 1.450 Mg/m^3.

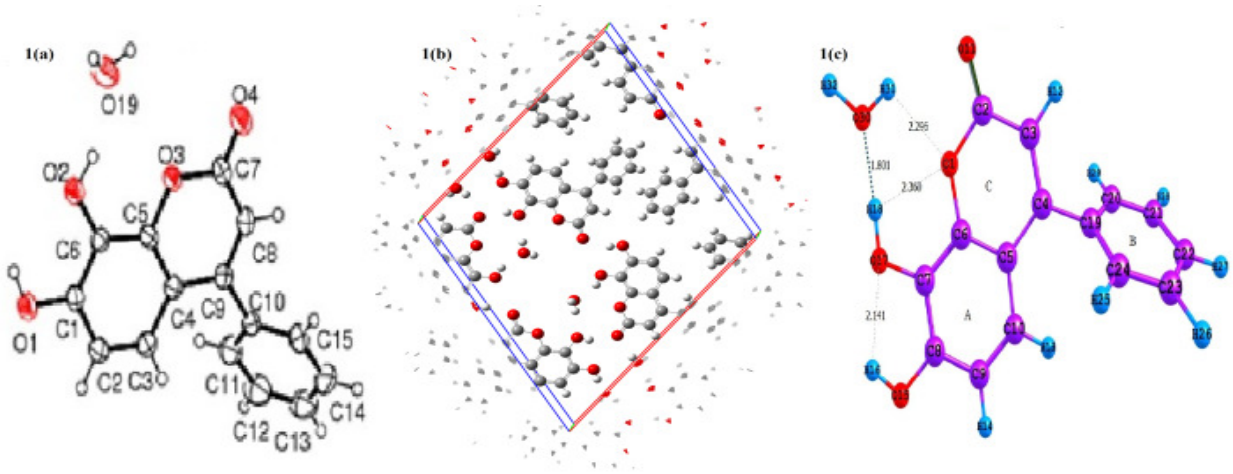

Figure 1 (a) Ortep diagram (b) Crystal pack diagram (c) Optimized geometry of DHPC

DHPC molecule exists in monoclinic system with $P2_1/c$ space group, exhibiting lattice and unit cell parameters α= 90°,β= 107.556(2)°,γ = 90° and *a* = 19.2293(10) Å, *b* = 14.5079(8) Å, *c*=18.7494(10) Å, respectively. The data was deposited on the Cambridge Crystallographic Data Centre [**CCDC No. 1486677**]. Figure 1(a) shows ORTEP diagram while figure 1(b) represents the crystal pack diagram and figure 1(c) optimized molecular structure of DHPC.

TABLE 1. CRYSTAL DATA AND STRUCTURE REFINEMENT FOR DHPC	
Empirical formula	C15 H12 O5.H_2O
Formula weight	272.25
Crystal system	Monoclinic
Temperature	296(2) K
Wavelength	0.71073 Å
Space group	$P2_1/c$
Unit cell dimensions	a = 19.22 (10) Å ; α= 90°. b = 14.50 (8) Å ; β= 107.55 (2)°. c = 18.74 (10) Å ; γ = 90°.
Volume	4987.0(5) $Å^3$
Z	16
Density	1.450 Mg/m^3
Crystal Size	0.300 x 0.250 x 0.200 mm^3
Index Range	-22<=h<=22, -17<=k<=17, -22<=l<=17
Largest diff. peak and hole	0.32 and -0.24 $eÅ^{-3}$

4.3 Geometry optimization

Structural optimization at ground state level of DHPC have been performed using B3LYP/6-311++G(d,p) basis set. Optimized structural parameters along with crystallographic bond parameters are summarized in Table.2. Bond length depends on the bond order, orbital hybridization and resonance or delocalization of π-electrons of a molecule. Crystallography has able to detect the arrangement of atoms within a crystal by the atom-induced diffraction of X-rays.

XRD analysis exposes intermolecular O-H...O hydrogen bonding concerned with hydroxyl groups and monohydrate molecule O2-H2A binds to monohydrate atom O19 with bond angle 154° and 2.65 Å bond distance. O19-H19B binds to ring oxygen atom, O3 with 2.60 Å at 173°. Intramolecular bonding exists in coumarin ring system O1-H1A...O2 = 2.72Å binds to neighboring hydroxyl group at C6 while O2-H2A binds to ring O3 (2.70 Å) with bond angle 108°.

Table 2. Crystallographic and optimized structural parameters of DHPC					
Bond Length(Å)			**Bond Angle (°)**		
Parameters	**Calc.**	**Expt.**	**Parameters**	**Calc.**	**Expt.**
O1-C2	1.38	1.36	C2-O1-C6	123.1	120.2
O1-C6	1.36	1.38	O1-C2-C3	115.7	117.9
C2-C3	1.44	1.41	O1-C2-O11	116.0	116.4
C2-O11	1.21	1.21	C3-C2-O11	128.2	125.6
C3-C4	1.36	1.34	C2-C3-C4	122.6	123.2
C4-C5	1.45	1.44	C3-C4-C19	119.1	118.7
C4-C19	1.48	1.48	C5-C4-C19	121.1	122.5
C5-C6	1.40	1.39	C4-C5-C6	116.8	117.2
C5-C10	1.40	1.39	C4-C5-C10	125.7	125.5
C6-C7	1.39	1.38	C6-C5-C10	117.4	117.1
C7-C8	1.39	1.39	O1-C6-C5	121.8	122.2
C7-O17	1.35	1.34	O1-C6-C7	115.4	114.4
C8-C9	1.39	1.38	C5-C6-C7	122.6	123.3
C8-O15	1.35	1.35	C6-C7-C8	118.1	117.4
C9-C10	1.38	1.37	C6-C7-O17	124.9	125.3
C9-H14	1.08	0.93	C8-C7-O17	116.9	117.2
C10-H13	1.08	0.93	C7-C8-C9	120.5	120.6
O15-H16	0.96	0.85	C7-C8-O15	119.5	120.9
O17-H18	0.98	0.85	C9-C8-O15	119.9	118.3
C19-C20	1.40	1.38	C8-C9-C10	120.3	120.5
C19-C24	1.40	1.39	C5-C10-C9	120.7	120.8
C20-C21	1.39	1.37	C4-C19-C20	120.1	120.2
C20-H29	1.08	0.92	C4-C19-C24	121	121.4
C21-C22	1.39	1.37	C20-C19-C24	118.8	118.1
C21-H28	1.08	0.93	C19-C20-C21	120.5	120.9
C22-C23	1.39	1.36	C20-C21-C22	120.1	119.6
C22-H27	1.08	0.93	C19-C24-C23	120.4	120.5
C23-C24	1.39	1.37	O11-H31-O30	164.0	126.9
C23-H26	1.08	0.93	O1-H31-O11	55.46	38.8
C24-H25	1.08	0.93	O1-H31-O30	109.2	89.8
O30-H31	0.96	0.84	H31-O30-H32	106.9	110.5
O30-H32	0.96	0.83	H18-O30-H31	108.6	120.9
O1- H31	2.29	3.07	H18-O30-H32	130.9	121.4
O30-H18	1.80	1.86	O17-H18-O30	174.0	97.5

Deprotonation and proton transfer from hydroxyl group to monohydrate molecule results strong intermolecular hydrogen bonding O30-H18…O17 and O30-H31…O1 have donor-acceptor distance 2.7Å. Moreover two strong intramolecular hydrogen bonds O15-H16···O17 and O17–H18···O1 have donor-acceptor distances of 2.68 and 2.7 Å [30] has been revealed by optimized molecular geometry of electronic energy -955.2426 Hartree, which is supported by van der Waals radii (2.5Å) [31]. Table 3 show crystallographic and optimized hydrogen bonding interactions of DHPC.

Table 3. Hydrogen bonding interactions of DH4PC

Donor H…Acceptor	D-H	H…A	D…A	D-H…A
CRYSTALLOGRAPHIC DATA				
O2-H2A...O19	0.85	1.91	2.6	154
O19-H19B...O3	0.86	1.74	2.6	173
O1-H1A...O2	0.85	2.31	2.7	110
O2-H2A...O3	0.85	2.35	2.7	108
OPTIMIZED STRUCTURE DATA				
O30-H18…O17	0.98	1.91	2.65	154
O30-H31…O1	0.84	1.8	2.7	174
O15–H16···O17	0.96	2.14	2.68	113
O17-H18···O1	0.98	2.35	2.75	103

4.4 Spectral Vibrational Analysis

DHPC has 32 atoms and 90 normal modes of vibrations distributed according to group theory analysis as: Γ_{vib}= 61À + 29 Ä. Vibrations of type À belong to in-plane (planar) and those of type Ä belong to out of plane (non-planar) mode. In the absorption spectra, some wavenumbers are assigned twice to different normal modes of the molecule (Table 4). Observed and simulated FT-IR and FT-Raman spectra of the title compound, which helps to understand the observed spectral features shown in figure 2a and 2b.

4.4.1 C-H Vibrations

C-H stretch vibrations are generally observed in the range 3100-3000 cm^{-1} giving rise to multiple band [32] and these bands are observed as very weak bands with calculated/ experimental value 3147/3145 cm-1, 3155/3156 cm-1, 3169/3170 cm-1 in Raman with PED(99%). C-H in-plane and out-of-plane bending vibrations expected to lie in the region 1500-1100 cm-1 and 1000-750 cm-1 [33], respectively occur at 1374, 1355,1305,1268,1210 cm-1 in FT-IR (In-plane) as medium

bands and at 1067 (weak), 1107 (weak), 1251 (strong), 1373 (strong), and 1461 (medium) cm-1 in Raman. PED shows that C-H stretching are pure modes while the C-H in-plane bending vibrations are mixed with 10-30% of CCC in-plane bending modes and vice versa. Weak bands at 908, 918, 808 cm-1(IR) and at 972 cm-1 (Raman) are assigned for C-H out-of-plane bending vibrations [34-35].

Table 4. Selected vibrational assignments of DHPC by normal coordinate analysis based on SQM force field calculations

Observed fundamentals (cm^{-1})		Selective scaled B3LYP with 6-31++G(d,P) force field	
υ_{IR}	υ_{Raman}	υ_{cal} cm^{-1}	Assignment (PED%)
3802,w		3800	ν_{AS} OH(55), ν_{SS}OH (45)
3718,w		3714	νOH II (100)
	3670,w	3671	ν_{SS}OH (54), ν_{AS} OH (45)
3398,vs		3396	νOHII (96)
	3187,w	3188	νCHII (99)
	3170,w	3169	νCHII (99)
	3156,w	3155	νCH III (99)
	3145,w	3147	νCH III (99)
1690,vs		1692	ν_{db}COI (47), νCCI (15), νCCII(14)
1667,vs		1669	βOH_{def} (82)
1655,s	1656,m	1657	νCC III (66), βCH III (17)
1635		1631	νCC III (61), βCH III (14), νCCII(6)
	1599vs	1596	νCC I(43), νCC II (12)
1566s	1563,m	1564	νCC II (19), τOH_B (17), τCOH (15), βCH2(10)
1510,m		1513	βCH III (49), νCC III (38)
	1461,m	1464	βCHIII(42), νCC III(32)
1374,m	1373,s	1376	βCHII(13),νCCI(12),τOH4 (12), τCOH(10)
1355,m		1356	νCC III (71), βCH III (28)
	1340,vw	1342	τOH_B (27), νCOII(12), νCCII (10)
1305,m		1307	βCH III (37), νCC III (31)
1284,m	1286,w	1286	τOH_B(25),νCCII (11),βCOH(10), νCOII (10)
1268,m		1264	νCC III (26), βCH II (13), βCH I (12)
	1251,vs	1250	βCH I (30), βCH II (22)
1240,m		1239	βCOH(25), νCCII(14),τOH_B (13), τCOH (11)
1210,m	1206,m	1208	βCH III (82), νCC III (17)

1179,m		1178	νCO I (30), νCC I(25)
	1107,w	1100	νCC III (43), βCH III (41)
1070,m		1071	τOH_B (15), νCO I (15), τCOH (13)
	1067,w	1062	νCC III (38), R_{TD} III (37), βCH III (21)
1035,m		1037	νCC III (51), gCH III (13), R_{TD} III (13)
1023,m	1026,m	1021	R_{ASYT} III (45), R_{ASYTO} III (31)
1001,vs		1000	R_{TD} II (19), νCC III (17), R_{TD} I (12)
918,w		916	gCH I (77)
908,w		908	gCHII (68), R_{ASYTO} III (10)
870,w		877	τOH_B (34), τCOH (29), COI(12)
808,w		806	τOH_B (46), τCOH (38), gCH III (19)
762,w	760,w	760	τOH_B (46), τCOH (36)
619,vw	619,vw	620	R_{PUK}III (44), R_{ASYTO} III (31)
606,vw		608	gCOI (20), R_{ASYT} II(17), R_{PUK}III (13)
530,vw		530	R_{PUK}III (32), R_{ASYT} III (23)
505,w	509,w	505	τOH_B(31), OH_B (16), OH_{rock} (13)

vs: verystrong; s: strong; m: medium; w: weak; υ: stretching; β: bending; db: double bond.

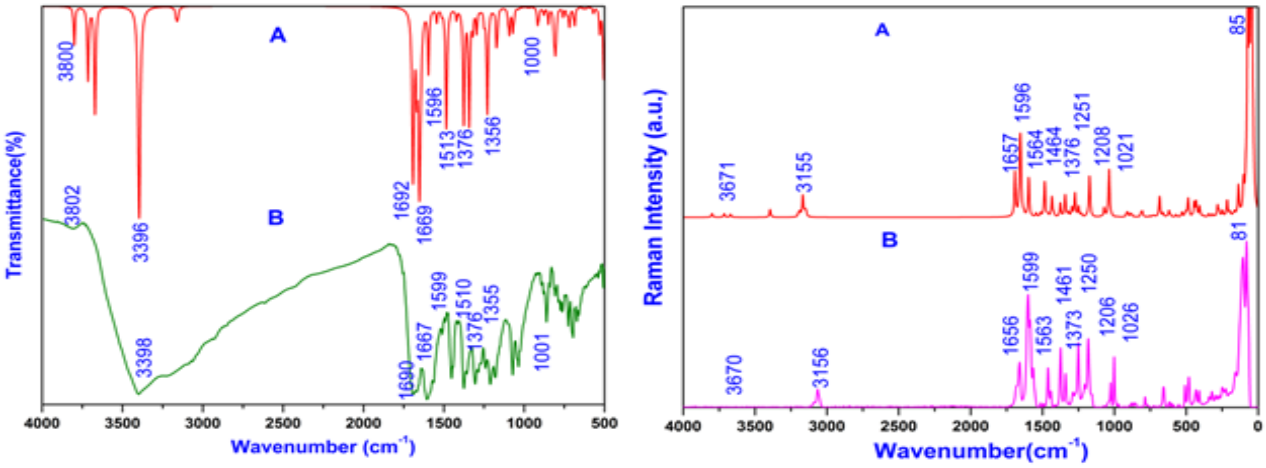

Figure 2 (a) FT-IR Spectra of DHPC **2** (b) FT-Raman Spectra of DHPC A).Simulated B).Experimental

4.4.2 Red shifting O-H…O Vibrations

Free O-H hydroxyl stretching vibration generally occurs in the region 3500-3700 cm^{-1} [36] and due to field effect, frequency lowers and intramolecular hydrogen bonding red shifts O-H stretching wavenumber to the region 3550-3200 cm^{-1}. Computed wavenumber by DFT level at 3396

cm^{-1} and a strong sharp band at 3398 cm^{-1} assigned to O-H stretching mode vibration. Generally O-H in-plane bending modes appear as strong bands in the region 1440-1260 cm^{-1} [37-40] that are viewed at 1284 cm^{-1} (IR) and at 1340, 1286 cm^{-1} (Raman) laterally with C-H in-plane and C-C stretching vibrations. Weak intensity characteristics band due to out-of-plane bending assigned at 344 cm^{-1} in Raman [41,42]. O-H deformation modes of bonded monohydrate molecule observed as very strong band at 1667 cm-1 and torsional modes as medium bands at 1284, 1240, 1070 cm^{-1} in IR. Weak bands at 870, 808, 762cm^{-1} and at 1340, 1286cm^{-1} in IR and Raman, respectively are also noted.

4.4.3 C-C Vibrations

C-C stretching (ring) vibrations of coumarin have characteristic bands in both IR and Raman spectra, covering the spectral range from 1610 to 1300 cm^{-1} [43-44]. Medium intensity band assigned in IR at 1510, 1374, 1355, 1305 cm^{-1} and in Raman band at 1563, 1461cm^{-1}. Among the calculated bands strong bands at 1566 (IR) and 1373 cm^{-1} (R) and very strong Raman band at 1599 cm^{-1} is attributed to νC-C vibrations. Benzene ring C-C stretching vibrations attributed to 1655, 1635, 1268, 1035, and 1001 cm^{-1} in IR and 1656, 1206, 1107 and 1067 cm^{-1} in Raman spectrum.

4.4.4 C=O Vibrations

Characteristic peak in IR spectrum for the C=O stretching frequency of coumarin is usually observed in the region 1700 to 1750 cm^{-1} [44]. Observed C_2=O_{11} stretch mode shifts to a frequency lower than 1700cm^{-1} and a very strong absorption band at 1690 cm^{-1} with a red shift of ≈10 cm^{-1} is observed in IR. DFT calculations locate this mode at 1692 cm^{-1}. Resonance effect, thereby conjugation and greater masses of attached atoms lowers the IR frequency at which the bond will absorb. Deformation bands of C=O expected in the regions 625 ± 70 and 540 ± 80 cm^{-1}, respectively [44] are observed at 606, 564 cm^{-1} in IR and at 344 cm^{-1} in Raman with weak intensity. In both spectra, weak band at 725 cm^{-1} are assigned to C=O out-of-plane bending vibrations. Sadia Rehman *et al*. [45] assigned a weak band in the range of 1090-1120 cm^{-1} as the stretching frequency of C-O of lactone ring. A medium band in IR spectra at 1179 cm^{-1} with PED (30%) occurs in phenyl ring attached to coumarin moiety.

4.5 Thermogravimetric and Differential Thermal Analysis

Thermal analysis of DHPC has been done in solid phase and TG and DTA thermogram of DHPC is shown in Fig 3. Single stage decomposition curve shows that compound is almost stable up to 220°C and starts major decomposition after heating beyond 220°C. The first weight loss occurs in the temperature range 97°C amounting to 6% weight loss due to the loss of solvent molecule present in it and the second one between 97 and 348°C which amounts to the rest of the sample 94%. There is no residue observed for the sample as the compound completely decomposed at 348°C.

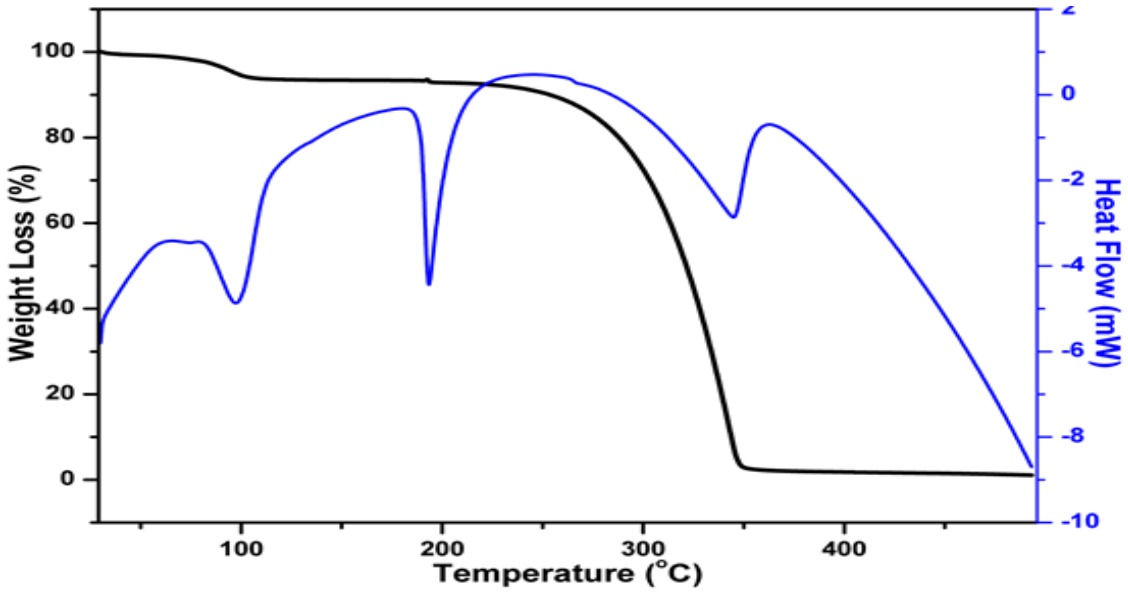

Figure 3 Experimental TG and DTA Curves of DHPC

TG curve suggests that simultaneous melting and decomposition of DHPC occur in the temperature range 97 to 350°C. DTA thermograms also reflect the decomposition at temperatures 97°C and 350ºC. Endothermic dip at 193°C is due to the melting point of the compound and endothermic dip at 350°C acknowledges thermo-oxidative (certain content of O_2) decomposition of the compound [46].

4.6 Thermal Property Analysis in Gas Phase

Thermodynamic functions: heat capacity (C°p.m), entropy (S°m) and enthalpy changes ($\Delta H°_m$) for DHPC molecule were computed from the theoretical harmonic frequencies and tabulated in Table 5. Computed thermodynamic parameters increase with increase in temperature ranging from 100 to 1000 K due to the fact that, the molecular vibrational intensities increase with increase in temperature [47]. Correlation equations between heat capacity, entropy, enthalpy changes and temperatures were fitted by quadratic formulas and the corresponding fitting factors (R^2) for these thermodynamic properties are 0.9994, 0.9999and 0.9993, respectively. Thermochemical field can use these parameters to compute the other thermodynamic energies and estimate directions of chemical reactions according to relationship of thermodynamic functions and using second law of thermodynamics. All thermodynamic property calculations done in gas phase and they could not be used in the solution. The corresponding fitting equations (1-3) are as follows and the correlation graphics are shown in Fig 4.

$$C°p.m = 5.24+0.263T-0.00001T^2 \quad (R2 = 0.999) \ldots. \quad (1)$$

$$S°m = 58.98+0.291T-0.00007T^2 \quad (R2 = 0.999) \ldots. \quad (2)$$

$$\Delta H°m = -3.74+0.036T-0.00006T^2 \quad (R2 = 0.999) \ldots. \quad (3)$$

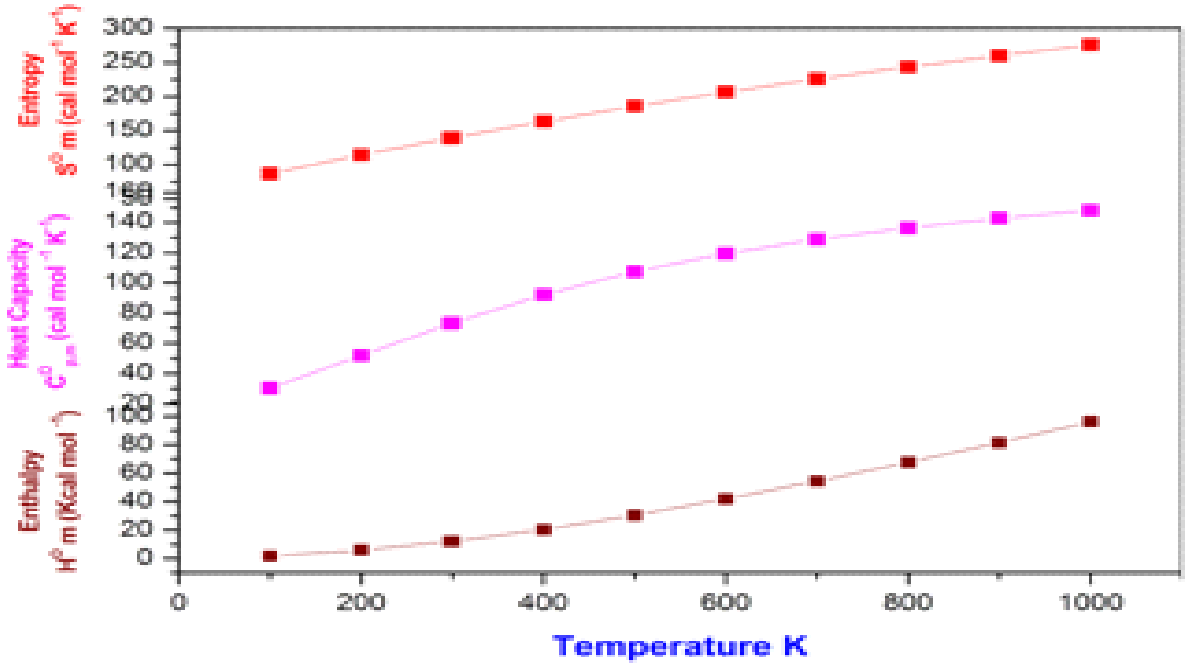

Figure 4 Correlation graphs of thermodynamic properties at different temperatures for DHPC

Table 5: Thermodynamic parameters of DHPC

TEMPERATURE T (K)	HEAT CAPACITY Cp (cal/mol.K)	ENTROPY S (cal/mol.K)	ENTHALPY ΔH (kcal/mol)
100	30.26	86.90	1.88
200	52.03	114.51	5.99
298.15	73.12	139.27	12.14
300	73.50	139.72	12.28
400	92.32	163.53	20.60
500	107.52	185.83	30.62
600	119.47	206.53	41.99
700	128.91	225.69	54.43
800	136.53	243.42	67.72
900	142.78	259.87	81.69
1000	148.00	275.19	96.24

5. Conclusion

Neoflavonoid 7,8 dihydroxy 4-phenylcoumarin monohydrate crystallizes in the monoclinic centrosymmetric space with z=16 concludes a complete structural, vibrational, electronic and thermodynamic analytical studies of DHPC that have been carried out with spectroscopic techniques along with DFT method. Scaled frequency calculation agrees satisfactorily with the experimental interpretations confirming inter and intra-molecular hydrogen bonding interactions. Thermal analysis shows that title compound is thermally stable up to 220°c and physiochemical properties attribute its bioactive significance. Linear correlation graphs between heat capacity, entropy, enthalpy changes and temperatures fitted by quadratic formulas increases with temperature.

REFERENCES

[1] Mariusz Tasior *et al. J. Org. Chem.* **79(18)** 8723 (2014).

[2] Rashid Nazir, Anton J.Stasyuk, Daniel T.Gryko *J.Org.Chem.* **81(22)** 11104 (2016).

[3] J.B Hudson, E.A Graham, L Harris, M.J Ashwood-Smith *J. Photochem Photobiol*. **57(3)** 491 (1993).

[4] Kimura Y, Okuda H, Journal of Natural Products 249-251 (1997).

[5] Bubols G.B *et al. Mini-Reviews in Medicinal Chemistry*. **13(3)** 318 (2013).

[6] Venugopala K.N, Rashmi V, Odhav B *BioMed Research International* 14 (2013).

[7] Donna L.Romero, Peter R. Manninen, Fusen Han, Arthur G. Romero *J. Org. Chem.* **64(13)** 4980 (1999).

[8] Zhao H, Neamati N, Hong H *J. Med. Chem.* **40** 242 (1997).

[9] J.B Veselinović, J.S Matejić, A.M Veselinović , D Sokolović *Biologica Nyssana.* **7 (2)** 167 (2016).

[10] T Adfa M, Itoh, Y Hattori, M Koketsu *Biol. Pharm. Bull.* **35(6)** 963 (2012).

[11] Stancho Stanchev, Frank Jensen, Ilia Manolov, International Journal of Quantum Chemistry **108 (8)** 1340–1351 (2008).

[12] D. Anitha Rexalin, Cauvery Research Journal, Volume **1(1)** 75-81 (2007).

[13] C.K. Johnson, M.N Burnett, ORTEP 3. Report ORNL-6895, Oak Ridge National Laboratory, Tennessee, USA, (1996).

[14] Louis J. Farrugia, J. Appl. Crystallogr. **32** 837-838 (1999).

[15] C.F. Macrae, P.R. Edgington, P. McCabe, E. Pidcock, G.P. Shields, R. Taylor, M. Towler, J. van de Streek J. Appl. Crystallogr. **39** 453-457 (2006).

[16] S.P. Westrip J. Appl. Crystallogr. **43** 920-925 (2010).

[17] P.C. Hariharan, J.A. Pople Theoretica Chimica Acta. **28** 213-222 (1973).

[18] R. Krishnan, J.S. Binkley, R. Seeger, J.A.Pople J. Chem. Phys.**72** 650-654 (1980).

[19] A.D. Becke J. Chem. Phys. **98** 5648-5652 (1993).

[20] A.D. Becke Phys. Rev. A.**38** 3098-3100 (1988).

[21] C.Lee, W.Yang, R.G. Parr Phys. Rev. B **37** 785-789 (1988).

[22] M.J.Frisch, G.W.Trucks, H.B.Schlegel, G.E. Scuseria, M.A. Robb, J.R.Cheeseman, G.Scalmani, V.Barone, B. Mennucci, G.A.Petersson, H.Nakatsuji, M.Caricato, X. Li, H.P.Hratchian, A.F.Izmaylov, J.Bloino, G.Zheng, J.L.Sonnenberg, M.Hada, M.Ehara, K.Toyota, R.Fukuda, J.Hasegawa, M.Ishida, T.Nakajima, Y. Honda, O.Kitao, H. Nakai, T.Vreven, J.A.Montgomery Jr., J.E. Peralta, F.Ogliaro, M.Bearpark, J.J. Heyd, E. Brothers, K.N. Kudin, V.N. Staroverov, T. Keith, R. Kobayashi, J. Normand, K.Raghavachari, A. Rendell, J.C.Burant, S.S.Iyengar, J.Tomasi, M. Cossi, N. Rega, J.M. Millam, M. Klene, J.E. Knox, J.B. Cross, V. Bakken, C. Adamo, J. Jaramillo, R. Gomperts, R.E. Stratmann, O.Yazyev, A.J.Austin, R.Cammi, C.Pomelli, J.W.Ochterski, R. L.Martin, K. Morokuma, V.G. Zakrzewski, G.A.Voth, P. Salvador, J.J. Dannenberg, S. Dapprich, A.D. Daniels, O.Farkas J.B. Foresman, J.V. Ortiz, J. Cioslowski, D.J Fox, Gaussian 09, Revision C.02, Gaussian Inc.: Wallingford, CT.USA, (2009).

[23] A.P.Scott, L. Radom J. Phys. Chem. **100** 16502-16513 (1996).

[24] J.B.Foresman, A. Frisch Exploring Chemistry with Electronic Structure Methods, 2nd Edn, Gaussian, Pittsburgh (1996).

[25] T. Sundius J. Mol. Struct. **218** 321-326 (1990).

[26] T. Sundius Vib. Spectrosc. **29** 89-95 (2002).

[27] P.Pulay, G. Fogarasi, G. Pongor, J.E.Boggs, A.Vargha J. Am. Chem. Soc. **105** 7037-7047 (1983).

[28] P. Pulay, G. Fogarasi, F. Pang, J.E. Boggs J. Am. Chem. Soc. **101** 2550-2560 (1979).

[29] K.K.Irikura, THERMO.PL, National Institute of Standards and Technology, (2002).

[30] Jeffrey, A.George, An introduction to hydrogen bonding, Oxford University Press (1997).

[31] L. Pauling, The nature of the chemical bond. Cornell University Press, New York (1960).

[32] Udaya Sri N, K.Chaitanya, M.V.S Prasad, Spectrochim Acta A **97** 728 (2012).

[33] S.B Doddamani, A. Ramoji, J. Yenagi, Spectrochim Acta A **67** 150 (2007) .

[34] J.R. Scherer, Spectrochim Acta A **21**:321 (1965).

[35] G.Thilagavathi, M. Arivazhagan, Spectrochim Acta A **79** 389 (2010).

[36] Rensheng Xu, Yang Ye, Weimin Zhao, Introduction to Natural Products Chemistry, CRC Press (2011).

[37] B. Smith, Infrared Spectral Interpretation: A Systematic Approach, CRC Press (1999).

[38] M. Narayana Bhat, S.M. Dharmaprakash, J. Cryst. Growth **236** 376-380 (2002).

[39] L.J. Bellamy, The Infrared Spectra of Complex Molecules, Chapman and Hall, London (1980).

[40] N.B. Colthup, L.H. Daly, S.E. Wiberley, Introduction to Infrared and Raman Spectroscopy, Academic Press, New York (1990).

[41] G. Socrates, Infrared and Raman Characteristic Group Wave Numbers- Tables and Charts, 3 rd Edition, John Wiley and Sons, New York (1980).

[42] Y. Erdogdu , M.TGulluoglu, Spectrochim Acta A **74** 162 (2009).

[43] G. Varsanyi, Vibrational Spectra of Benzene Derivatives, Academic Press, New York (1969).

[44] N.P.G RoegesA Guide to the Complete Interpretation of Infrared Spectra of Organic Structures, Wiley, New York (1994).

[45] Sadia Rehman, Muhammad Ikram, Ajmal Khan,Soyoung Min,Effat Azad, Thomas S Hofer, KH Mok,Robert J Baker,Alexander J Blake,Saeed Ur Rehman ,Chem Cent J. **7** 110 (2013).

[46] Michael Edwart Brown Introduction to Thermal Analysis: Techniques and Applications, New York: Kluwer Academic Publishers (2001).

[47] J. Bevan Ott, J. Boerio-goates, Calculations from Statistical Thermodynamics, Academic Press (2000)